Drastic reorganization of bioconvection pattern of *Chlamydomonas*: quantitative analysis of the pattern transition response

Azusa Kage, Chiharu Hosoya, Shoji A. Baba, Yoshihiro Mogami*

Graduate School of Humanities & Sciences, Ochanomizu University

Otsuka 2-1-1, Bunkyo-ku, Tokyo 112-8610, Japan

* Corresponding author.

Phone/Fax: +81-3-5978-5368

E-mail: mogami.yoshihiro@ocha.ac.jp

Key words: bioconvection, phase transition, gravitaxis, gyrotaxis

Summary

Motile aquatic microorganisms are known to self-organize into bioconvection. The swimming activity of the population of the microorganisms leads to the emergence of macroscopic patterns of density under the influence of gravity. Although long-term development of the bioconvection pattern is important in order to elucidate the possible integration of physiological functions of individuals through the bioconvection pattern formation, little quantitative investigation has been done. In the present paper, we present the first quantitative description of long-term behavior of bioconvection of *Chlamydomonas reinhardtii*, particularly focusing on the "pattern transition response." The pattern transition response is a sudden breakdown of the steady bioconvection pattern followed by re-formation of the pattern with a decreased wavelength. We found the three phases in the pattern formation of the bioconvection of *Chlamydomonas*: the *Onset*, *Steady State 1* before the transition and *Steady State 2* after the transition. In *Onset*, the wavelength of the bioconvection pattern increases with increasing depth, but not in *Steady States 1* and *2*. By means of the newly developed two-axis view method, we revealed that the population of *Chlamydomonas* moves toward the bottom of the experimental chamber just before the pattern transition. This fact indicates the pattern transition response could be caused by enhancing the gyrotaxis of *Chlamydomonas* due to the changes in the balance between the gravitactic and gyrotactic torques. We also found that the bioconvection pattern changes in response to the intensity of red-light illumination, to which *Chlamydomonas* is phototactically insensitive. These facts suggest the bioconvection pattern has a potential to drastically reorganize its convection structure in response to the physiological processes under the influence of the environmental cues.

Introduction

Bioconvection is a phenomenon of macroscopic pattern formation which occurs as a result of the collective motion of the swimming microorganisms. Starting from the well-mixed homogeneous suspension, swimming activity of the microorganisms biased by the gravitational force causes the anisotropic, top-heavy vertical stratification of the organisms. The accumulation of the organisms is then fragmented, forming downward plumes of the organisms. This fragmentation leads to a patch-like horizontal variation of the population density. After this vigorous "onset" process, suspension enters a sort of "steady-state" in which the horizontal density variation leads to a formation of macroscopic patterns consisting of polygons or dots regularly arrayed in appearance when viewed from above. The steady-state pattern remains for hours or even for days (Wager, 1911), as long as the microorganisms are motile.

Researches on the bioconvection so far have been focused mainly on the "onset" process of the pattern formation. It is partly because this process appears so similar to that of the thermal convection that they are considered to be analyzed in terms of the physical principles. It is also probably because the "steady-state" pattern that follows the onset process might be considered to be a kind of "static" state, in which the upward and the downward movement of the population of the organisms is in balance.

The steady-state bioconvection, however, is not in the static state, but has been demonstrated to dynamically respond to external stimuli. Mogami et al. (2004) demonstrated that the steady-state bioconvection pattern of the ciliate *Tetrahymena* responded to the changes in gravity acceleration. The pattern wavelength reduced with increasing acceleration. They also showed that the gravity-dependent response was different among the species and the behavioral mutants of the ciliate. This strongly

indicates that the motile properties of individual cells are integrated in the macroscopic response: bioconvection of *Tetrahymena* responded to altered gravity not just as isolated individuals, but as a system. From this fact, the speculation arises that physiological functions of the individual cell other than motility may be integrated through the collective movement of the population under the influence of gravity. That is, it is likely for bioconvection to play a role in physiology of microorganisms, for example, cell proliferation and mating, through generating macroscopic fluid flows.

In order to gain an insight into the role of bioconvection in biological events, quantitative analysis of the macroscopic behavior should be helpful. Detailed analyses on the temporal as well as spatial properties of the bioconvection pattern may reveal the ability of the macroscopic pattern to respond to the environmental cues, as shown in the case of gravity response. Quantitative analyses (e.g. Bees & Hill, 1997; Williams & Bees, 2011a), however, have so far tended to focus on the onset and relatively short-term behavior (i.e. <10 min from the onset), and the long-lasting, steady-state pattern has been analyzed largely in qualitative way (e.g. Wager, 1911, Yamamoto et al., 1992).

In the previous paper, through a long-term (> 10 min) observation of the steady-state bioconvection of *Chlamydomonas reinhardtii*, Akiyama et al. (2005) reported a quite interesting behavior of the steady-state pattern. The behavior, which we call in this paper the “pattern transition response” instead of the former term of “pattern alteration response” used in Akiyama et al. (2005), is a sudden decrease in wavelength of the pattern already formed steadily in the suspension. The transition response occurs spontaneously, in a manner highly similar to the phase transition found in the physical events; a local transition event spreads all over the suspension. Such behavior of the steady-state

bioconvection pattern had not so far been reported through experiments and had never been predicted by theoretical studies.

The pattern transition response observed in *Chlamydomonas* suggests that the bioconvection pattern, even though seemingly stable, is not always in a steady-state condition in which the upward and the downward movement of the microorganisms are in balance. It seems rather likely that the pattern is in the state of instability that allows the bioconvection itself to play possible roles of biological function.

In the present study, we made the first quantitative description characterizing the whole process of pattern formation and transition through long-term (>120 min) observations on the steady-state bioconvection of *Chlamydomonas*. Through detailed observation over two hours, we determined the three phases of bioconvection of *Chlamydomonas*: *Onset*, *Steady State 1* before pattern transition and *Steady State 2* after the transition. Although the latter 2 phases are not strictly regarded as “steady-states,” we call these phases “Steady” for simplicity in the expression in this paper. We found that, in *Onset*, the pattern wavelength increases with increasing depth, but not in *Steady States*. Second, through vertical-horizontal simultaneous observations (two-axis view), we demonstrated that just before the pattern transition occurs, most of *Chlamydomonas* cells move toward the bottom of the experimental chamber. Finally, we showed that changing the time-averaged intensity of red light can change the pattern wavelength. This is the first quantitative report that red light affects bioconvection patterns, to which *Chlamydomonas* shows no phototaxis.

Material & Methods

Cell Culture

Chlamydomonas reinhardtii strain 137c mt- was kept gently aerated for 3 or 4 days in the sterile tris-acetate-phosphate (TAP) medium at 25 °C under 12 h:12 h light/dark cycle (photon flux density at light phase, ~120 μmol m^{-1} sec^{-1}). To obtain the suspension of a given cell density (1 to 10× 10^6 cells/ml), cells were counted on Fuchs-Rosenthal hemocytometer, and then diluted with fresh TAP (Akiyama et al., 2005). Experiments were carried out at the middle of the light phase and at ambient temperature of 20-26 ℃ (in most cases, around 24 ℃).

Plan-view observation

The cell suspension of a given density was transferred into a flat circular glass chamber of an inner diameter of 94 mm without an air gap between the top and bottom glass plates separated by plastic spacer of a given height (1 to 8 mm). For details, see Akiyama et al. (2005). For the description of the time course of the bioconvection pattern formation and its transient response, we defined time zero as the time when the transfer of the suspension was completed.

Top-view images of the bioconvection patterns were taken at the rate of 0.1 fps (i.e. 1 image per 10 sec) using the high-definition camcorder, HDR-HC1 (Sony, Tokyo, Japan). The image size was 1920 × 1440 pixels on a 256 gray scale.

The experimental chamber was illuminated from the bottom with a flat light viewer (MedaLight LP-100, Minato Shokai Co. Ltd., Yokohama, Japan). Wavelengths of <640 nm were cut out with a sharp cut filter, SC-64 (Fuji Film, Tokyo, Japan). Under such an illumination condition, *Chlamydomonas* is known to show no phototactic

response. Taken under transmissive illumination, the dark region of the obtained image corresponds to the region where *Chlamydomonas* densely accumulates.

For long-term recordings, we used intermittent lighting (noted as IL) in which the light was on for 3.3 sec during 10 sec of the recording interval to minimize the non-tactic photoresponse such as photosynthesis. In some experiments, continuous lighting (CL) was used to increase the time-averaged illumination intensity, which may regain the photoresponse. In order to reduce the illumination intensity, neutral density filters (ND-0.3, Fuji Film, Tokyo, Japan) were used in addition to the sharp cut filter. For the comparison of the effects of reduced illumination intensity, one cell suspension prepared from a single culture was divided and transferred into two separate chambers; one was illuminated with the neutral density filter and the other without a neutral density filter. Bioconvection patterns of these two chambers were recorded simultaneously under the same illumination source (Light Viewer 7000 PRO, Hakuba Photo Industry Co. Ltd., Tokyo, Japan) with the photon flux density of 1 μmol m^{-1} sec^{-1} (light intensity: 20 lux without a ND filter).

Image Analysis

For plan-view observations, pattern wave numbers were calculated using the 2D-FFT method (Bees & Hill, 1997; Mogami et al., 2004). For the individual image of the bioconvection pattern, 2D-FFT was conducted with a lab-made image analysis software, Bohboh (Bohbohsoft, Tokyo, Japan), and the Fourier spectrum was obtained. To calculate the representative value of the wave number (spatial frequency) of an image, a Gaussian function was fitted to the Fourier spectrum using the least-square method. The peak value of the Gaussian function was regarded as the dominant wave

number of the image, i.e. reciprocal of the wavelength of the pattern. In the following, "wave number" refers to the dominant wave number, for simplicity.

In order to grasp the bulk motion of *Chlamydomonas*, we used the space-time plot method as in Kage et al. (2011). Following the method introduced by Mogami et al (2004), a narrow rectangular region was cut out from a stack of images and then pasted together following the time sequence. The space-time plot has the dimension of time and space, representing the temporal change of the given region.

Two-axis view

To examine the vertical as well as the horizontal movement of *Chlamydomonas* population, we developed the two-axis view system (Fig. 1), in which we can observe bioconvection from the top and from the side simultaneously. A quartz glass cell of inner dimensions, 3 mm height × 3 mm depth × 40 mm width, was used as an experimental chamber. Two cold cathode fluorescent lamps were used as light sources, which were arranged to pass light through a ~0.5-mm slit with a sharp cut filter SC 64. Top- and side- view images obtained with CCD cameras (XC-ES50, Sony, Tokyo, Japan) were mixed with a multiviewer (MV-40F, FOR-A Company Ltd., Tokyo, Japan), and recorded with a recorder (D-motion DVR-2100, Asiacorp International Ltd., Hong Kong) at a rate of 30 fps and of an image size of 640 × 320 pixels. In this way we can synchronize the top- and the side-view images.

Statistics

In order to assess the effect of suspension depth and cell density on the wave number of the convection pattern, we used the Kruskal-Wallis test, a nonparametric

counterpart of the one-way ANOVA. In addition, in order to know whether the values show an increasing or a decreasing trend, we used the Spearman's rank correlation. In the following, r_s denotes the Spearman rank correlation coefficient. The statistical processing was done with R (www.r-project.org).

Results

Pattern formation and the spontaneous pattern transition response

As reported in the previous paper (Akiyama et al, 2005), we found a dynamic behavior of the bioconvection pattern of *Chlamydomonas reinhardtii*. It was revealed in the frame-by-frame analysis of long-period (> 30 min) recordings in which the bioconvection pattern suddenly changed its wavelength. We call this transient change "pattern transition response," which was formerly called "pattern alteration response" in the previous paper.

Fig. 2 and Movie S1 shows a typical example of bioconvection pattern formation of *Chlamydomonas reinhardtii*. Sequential images of the plan views of the bioconvection pattern and the corresponding changes of wave number of the pattern image assessed by 2D-FFT are shown in Fig. 2A and B, respectively.

The pattern emerged in the well-mixed homogeneous suspension (Fig. 2A, 0 min) as a local accumulation of the cells in rectilinear pattern (Fig. 2A, 0.5 and 1 min). This onset pattern gradually changed its shape, and grew to a stable pattern, a regular array of dark dots surrounded by bright reticular lines (Fig. 2A, 5, 18 and 21 min). For several (sometimes several tens of) minutes this pattern was kept in a steady state, then a vigorous change occurred. The latter was observed as a local change of the steady-state pattern, in which the dark dots in the stable pattern spontaneously fragmented into smaller dots (Fig. 2A, 22 min, left side). This fragmentation of the pattern unit propagated throughout the suspension (Fig. 2A, 22, and 23 min). From the fragmented, less-organized state (Fig 2A, 24, 25 and 28 min), another stable pattern was formed (Fig. 2A, 30 and 40 min), and remained stable for more than a couple of hours as long as the cells were motile (Fig. 2A, 60 and 90 min).

The wave number of the plan-view image was small at the onset of the bioconvection pattern and gradually increased to reach a plateau, corresponding to the formation of the stable bioconvection pattern. The number suddenly increased further to another plateau through a spike-like transient, corresponding to the transition between steady-state patterns through the propagation of the spontaneous fragmentation of the convection cell.

The transitional event of the bioconvection pattern in the bulk of the *Chlamydomonas* suspension is summarized in the space-time plot (Fig. 2C). The plot, so-called kymographic or slit camera presentation, shows two regions with distinct spacing of stripes, representing the pattern transition response in the wavelength of the bioconvection pattern. Between these regions there exists a transitional zone where the stripes appear disordered. The beginning of this transitional zone is slightly delayed in the upper part of the figure, which indicates the propagation of the transitional event (Fig. 2B, 22 to 23 min).

In the present paper we focused our attention on the bioconvection pattern of the three remarkable phases; *Onset* and the two steady states, *Steady State 1* (SS1) and *Steady State 2* (SS2), before and after the transition, respectively. These three phases are marked in Fig. 2B.

Fig. 3 summarizes the measurement of the wave number of the convection pattern at the three different phases. Values were obtained from the separate experiments of fixed parameters (suspension depth of 4 mm and the cell density of 1×10^7 cells/ml). Under these conditions, the spontaneous pattern transition response occurred after 10.2 ± 7.5 min (mean ± standard deviation, n=18) from time zero. The wave numbers measured in the SS1 and SS2 showed a larger variation among samples than those

measured in the *Onset*, but no significant correlation was found between the wave numbers of the onset pattern and those of the steady-state patterns (Fig. 3A). However, wave numbers of the SS1 and SS2 showed a significant correlation at the 5% significance level (Fig. 3B, R=0.59, p=0.015, Pearson's product moment correlation, n=16). Wave numbers of the SS2 was about 1.4-1.8 times larger than those of SS1. This tendency was maintained irrespective of the depth and the density of cell suspension. In some cases (2 out of 18 experiments), the transition occurred so quickly that we could not confirm the SS1 before the transition.

Bees and Hill (1997) have reported that both the depth and the density of cell suspension has an effect on wavelength of "initial" and "final" patterns of bioconvection. We examined the effect of these factors on long-term behavior, including pattern transition response. The wave number of the onset pattern (Fig. 4A) showed clear decreasing trend with increasing suspension depth (Spearman's rank correlation test, $r_s \approx -0.9$, $p < 10^{-4}$ for all the density conditions), as reported in Bees & Hill (1997). On the other hand, the effect of suspension depth was different in the pattern of the SS1 and SS2. p-values by the Kruskal-Wallis test shown in Fig. 4B indicate that the wave number of the pattern in the SS1 and SS2 was likely to be insensitive to the changes in the suspension depth. .

Cell density of the suspension was less effective on the wave number of both onset and steady-state patterns. The onset pattern wave number did not show any clear increasing or decreasing trend with increasing density, except for the slight increasing trend of the suspension-depth condition of 2 mm (p=0.0036, Kruskal-Wallis test; $r_s = 0.68$, $p<10^{-4}$, Spearman rank correlation). Wave numbers of the SS1 and SS2 tended to increase with increasing cell density, although not always with statistical significance

(for SS1 and SS2, three or one out of the four different suspension depth conditions showed statistical significance, respectively; at 5% significance level, Kruskal-Wallis test). For the data sets which showed significance in the Kruskal-Wallis test, we calculated the Spearman rank correlation coefficient and its p-value. As a result, the coefficients were around 0.7 and the p-values were less than 0.01.

On the other hand, the effect of the cell density was clearly found on the initiation time of pattern transition response. When lowering the density, the transition occurred significantly later (Fig. 5). Suspension depth had little effect on the initiation time of pattern transition response ($p>0.1$ for each cell density condition, Kruskal-Wallis test).

Two-axis view

Since the development of the two-dimensional pattern is the result of the vertical convection of the cell population, the analysis of the vertical movement is required for understanding the basic mechanism of the pattern transition response. Several trials have been made to analyze the vertical convective movement (Harashima et al., 1988; Kitsunezaki et al., 2007). In these experiments, the vertical movement was solely assessed with no combination with the horizontal development of the bioconvection pattern. In the present study, we introduced an observation method which makes possible the simultaneous recording of the horizontal and vertical movement of the cell population.

Previously we used a quasi-planer vertical chamber for the observation of the vertical convective movement (Hosoya et al., 2010; Kage et al., 2011). In the narrow chamber (1 mm of width), downward plumes were formed in the suspension of

Chlamydomonas as well as *Tetrahymena*, which allowed us to observe the vertical movement of the cell populations. In altered gravity during the parabolic flight, the plumes were observed to change their shapes and the position in the chamber in response to the changes in gravity acceleration (Kage et al., 2011).

Although the horizontally narrow configuration of the chamber is useful for the quantitative observation of the plumes, the pattern transition response hardly occurs in such a narrow chamber. In the present study, we increased width of the vertical observation chamber to 3 mm, comparable to the spacing of the pattern developed horizontally in a Petri dish (see below), so that the pattern transition events were reproducibly induced and recorded in horizontal as well as vertical directions simultaneously through the flat glass walls (Fig. 1). An example of the whole recording is shown in Movie S2.

In the horizontal observation (Fig. 6A, left column), pattern formation was initiated near the wall of the chamber (Fig. 6A, Horizontal Observation, 2 min). Then the pattern reached a steady state (Fig. 6A, Hotizontal Observation, 5 min), although the shape of the pattern was not identical to that of the *Steady State 1* described above (Fig. 2A). Hereafter, the pattern began to change; the center of the aggregation blob became sharper, and then blobs became fragmented (Fig. 6A, Horizontal Observation, 10-14 min). Later the pattern reached the new steady state where the pattern wavelength decreased compared with the former steady state. This behavior is quite similar to the pattern transition response observed in the conventional flat horizontal chamber. In the present chamber configuration, the transition initiated 20.6 ±13.1 minutes after the experiment started (mean ± S.D., N=5). In relation to the two-dimensional observation, we call these two states *Steady State 1* (SS1) and *Steady State 2* (SS2) before and after

the transition, respectively.

Vertical observation (Fig. 6A, left column) showed that the onset of pattern formation occurs after the accumulation of the cell at the top of the chamber (Fig. 6A, Vertical Observation, 0 - 2 min) as reported in the previous observations (Hosoya et al, 2010; Kage et al, 2011). It also showed that, in the SS1, the “bottle-shaped” settling blobs are formed (Fig. 6 A, Vertical Observation, 5 min) as reported previously (Hosoya et al, 2010; Kage et al, 2011). At the moment the pattern transition response occurred (Fig. 6A, Vertical Observation, 10-14 min), the “neck” of the bottle-shaped blobs became constricted, and then a large portion of the *Chlamydomonas* cells migrated downwards, corresponding to the fragmentation of blobs in the horizontal observation. In the SS2 attained after the downward migration, the number of settling blobs increased compared with the SS1 (Fig. 6 A, Vertical Observation, 25 min). Average spacing between settling blobs was 3.42 ± 0.40 mm (mean ± S.D., N=5) and 1.79 ± 0.27 mm for SS1 and SS2, respectively. These values agree well with the wavelengths (the reciprocal of the wave numbers) in the horizontal observation of the same depth and cell density condition (depth: 3 mm, density: 1×10^7 cells/ml), which were 3.30 ± 0.27 mm and 1.98 ± 0.24 mm for SS1 and SS2, respectively (N=3).

Space-time plots (Fig. 6B to D) also show that at the beginning of the pattern transition response, the cells moved abruptly downwards. This is clearly demonstrated by the emergence of the bright portion in the space-time plot obtained at the top region of the chamber (indicated by an arrow in Fig. 6B), which is due to the dispersal of the cells. In contrast, the plot obtained at the bottom region shows the dark portion corresponding to the accumulation of the cell (Fig. 6C).

Light intensity dependent changes in pattern wavelength

We found a rapid decrease in the wave number in the pattern in the SS2, when we changed the illumination conditions from intermittent lighting (IL) to continuous lighting (CL) (Fig. 7A). This change was reversible; the pattern wave number changed depending on the changes of the illumination conditions between IL and CL (Fig. 7B). In contrast to the spontaneous pattern transition response, this illumination-type-dependent change in the pattern wave number occurred without accompanying the spike-like transient increase in the wave number that was usually found at the beginning of the pattern transition response (a spike-like change of the wave number shown in Figs 2 and 7). It took 5-10 minutes for the pattern to adapt the altered illumination and to respond to the next change. The change in the pattern wavelength was observed to occur simultaneously over the suspension, so that we could not observe the propagation of the transition event, which was the second feature of the spontaneous pattern transition response shown above. The effect of the illumination conditions was restricted to the SS2. It was not found that the bioconvection pattern in the SS1 was affected by time-averaged light intensity.

In order to assess the effect of the illumination conditions on bioconvection pattern formation, we attenuated the light intensity using neutral density (ND) filters (Fig. 7C). In most cases (8 of 9 independent experiments), wave number of the SS2 was larger when light was attenuated with the ND filter (Fig. 7C; p=0.00047, paired t-test), while the wave numbers of the onset pattern and SS1 were not clearly affected (onset: p=0.12, steady state 1: p=0.55, paired t-test). The initiation time of pattern transition response seems to be little affected by the illumination conditions (p=0.098, paired t-test). In 3 out of 9 experiments, the pattern transition response occurred earlier in the

samples with the ND filter, as in Fig. 7C. In the rest 6, those without the ND filter preceded. The wave number of each phase and the time when the transition occurred are shown in Fig. 7D. Only the SS2 showed a significant difference in wave number (paired *t*-test), but the transition time did not show any significant difference. When the ND filter was inserted in the midst of the SS2 under the continuous lighting, the SS2 pattern wave number increased (120 ± 3% compared between those before and after insertion; mean ± SD; N=4). These findings indicate that changes in the wave number are largely due to the changes in time-averaged intensity of the light; the bioconvection pattern in the SS2 reversibly changes its pattern wavelength in response to the total amount of light per unit time.

Discussion

In the present paper we describe quantitatively the pattern transition response of *Chlamydomonas reinhardtii*. 2D-FFT analysis showed that the wave numbers of the steady-state pattern were almost insensitive to the suspension depth and the average cell density of the suspension, while that of the onset pattern was really sensitive to the suspension depth and decreased with an increase in the depth. This sensitivity of the wave number to the suspension depth and the cell density are generally in line with those of Bees and Hill (1997), which have reported that the onset wavelength increases with increasing depth and the "final" wavelength decreases with increasing density.

The difference in the sensitivity of the pattern wavelength to the suspension depth found between the onset and steady-state patterns could be explained in terms of the physical theories proposed so far. Bioconvection has been explained from the upward migration of the microorganism biased purely by its physical properties. There have been principally two theoretical models proposed for the formation of the bioconvection pattern, especially at the onset of the bioconvection.

The "density instability model" (Childress et al., 1975) can be regarded as a general model of bioconvection, irrespective of the species of microorganisms. The top accumulation of microorganisms as the result of negative gravitaxis causes the instability in the stratification of the fluid density. The dense, microorganism-containing fluid at the top of the water column starts to settle down. This settling motion induces the onset of the bioconvection which grows to the regular spatial patterns consisting of down-flow of the accumulated organisms and up-flow of the negative gravitactically swimming organisms.

The onset of bioconvection has also been explained by another theoretical model, termed "gyrotactic instability model." Gyrotaxis is a biased swimming behavior peculiar to some gravitactic microalgae such as *Chlamydomonas* (Kessler, 1985b). It causes the algae to reorient based on the torque due to vorticity in the shear flow (gyrotactic torque), in combination with the upward-orienting torque (gravitactic torque) generated possibly by the posterior shift of the center of gravity (Kessler, 1985b). As a result, gyrotaxis causes *Chlamydomonas* to move towards the down-flow and away from up-flow. This distinct swimming behavior leads to a local accumulation of the organisms, which would cause the instability to induce large down-flow of the organisms. In this model, bioconvection begins with random flows, and density instability is not always necessary for the initiation of the convection.

Hopkins and Fauci (2002) conducted numerical simulations of bioconvection, considering the effect of negative gravitaxis, gyrotaxis and chemotaxis. In their simulation work, microorganisms were treated as a discrete point source of mass, the movement of which was affected by the fluid flow governed by the continuous Navier-Stokes equation. The discrete representation of microorganisms, as a result, facilitated the direct evaluation of cell orientation induced by the torques of gravitactic, gyrotactic, and chemotactic origin. The simulation done with several ten thousands particles in the vertical plane demonstrated the initial overturning of the top-accumulation to form downward-going plumes. Simulations on the "purely geotactic" particles showed that the wave number, reciprocal of the plume spacing, decreased with an increase in the suspension depth, while it was less sensitive to the suspension depth in the simulation on the particles with gyrotactic as well as gravitactic features (cf. Tables 3 and 4 in Hopkins and Fauci, 2002). Simulations also showed that

the wave number was smaller in “purely geotactic” cells. These results of simulation suggest that the gyrotactic feature is a potential factor explaining the different characteristics found between the pattern of *Onset* and that of SS1 and SS2.

At the *Onset*, overturning of the cell accumulation was induced due to the instability of the top-heavy stratification. This overturning caused shear flow accompanied with falling plumes, and then initiated the gyrotactic behavior of the cell. The pattern at SS1 may be developed and maintained further under the mutual combination of the gyrotactic and the gravitactic features of the cell.

It is therefore likely that the pattern transition response was triggered by the alteration of the balance of gyrotactic and/or gravitactic features. In the two-axis view, the *Chlamydomonas* cells were observed to form steep, concentrated “beams” and move altogether downwards during the pattern transition response (Fig. 6). This behavior implies the enhancement of the gyrotactic feature of the cell resulting in the entrainment of cells into the downward flow as shown in Kessler (1986a). Hopkins and Fauci (2002) reported that gyrotactic particles falling to the bottom in a plume have “more of the tendency to stay near the bottom of the plume than the purely geotactic particles.” This tendency is in line with our observation that larger population of the cell tended to accumulate at the bottom in SS2 than in SS1 (Fig. 6A, 5 min and 15 min). In addition, the visualization of gyrotactic plumes at “pseudo-steady state” (cf. Fig. 9, Hopkins and Fauci, 2002,) appears much similar to our observation of the movement of cell population during the pattern transition response (Fig. 6A, 12-14 min).

Enhanced gyrotactic features may have forced the larger number of cells to be entrained to the downward plumes, which caused the cell population to shift downward. This may break down the SS1 pattern, and the new pattern may emerge from the

disordered, quasi-stable state as the regular pattern consisting of the “bottom-standing” plumes with narrower spacing, which is characteristically obtained from the simulated bioconvection of gyrotactic organisms (Ghorai & Hill, 2000). The entrainment of the cell to the downward plume would be accelerated with increasing the cell density of the suspension, and result in the shortening of the latent time to the initiation of the pattern transition response (Fig. 5).

As the gyrotactic instability model states, orientation of the organism toward the flow axis is assumed to be caused by both the gyrotactic and the gravitactic torque (Kessler, 1985b). The gyrotactic torque is generated depending on the vorticity. This torque makes organisms inclined toward the axis of the downward flow. The inclination angle is determined as a balance between the gyrotactic and the gravitactic torques (Kessler, 1985b, 1986b). Enhancement of the gyrotaxis means the increase in the inclination, which is brought about either by an increase of the gyrotactic torque or a decrease of the gravitactic torque.

If the flow velocity field is invariant, the gyrotactic torque increases when the overall geometry of the cell changes to increase the viscous drag coefficient for rotational motion (Kessler, 1986a; Berg, 1993). The gravitactic torque decreases, on the other hand, depending on the two different mechanisms (Mogami et al., 2001). One is based on the bottom-heavy, fore-aft asymmetry of the internal density that displaces the center of gravity posterior to the center of buoyancy. Another is on the bottom-large, fore-aft asymmetry of the overall shape that causes, in low Reynolds number conditions, upward reorientation during sedimentation because the larger posterior part sediments faster than the smaller anterior part of the organism (Roberts, 1970). In the theory of gyrotaxis of *Chlamydomonas* so far, only the density asymmetry has been highlighted because of the

fact that immobilized algae continued to orientate upward in the medium of the same density as the algae (Kessler, 1985b). This fact, however, does not exclude the contribution of the shape asymmetry because in the isodensity, non-sedimenting conditions the shape asymmetry fails to generate the torque while the density asymmetry remains functioning. For the valid distinction of the mechanisms, specimens should be immersed in the hyperdensity medium, in which shape asymmetry causes anterior-down rotation because the larger posterior part floats faster than the smaller anterior part, while the density asymmetry causes the same anterior-up rotation (Mogami et al., 2001). Hosoya et al. (2010) demonstrated “positive” gravitaxis and the resultant “reverse” (inverted) bioconvection of *Chlamydomonas* in the hyperdensity medium containing Percoll. This fact indicates that the fore-aft shape asymmetry dominantly generates the gravitactic torque in *Chlamydomonas* rather than the fore-aft density asymmetry. It is therefore highly likely that the changes of the shape asymmetry may act either to increase the gyrotactic torque or to decrease the gravitactic torque, both of which would lead to the enhancement of the gyrotaxis of *Chlamydomonas*.

The spherical cell body of *Chlamydomonas* seems hardly deformed because of the presence of the rigid cell wall. Projections of the flagella at the front end of the cell body, in contrast, may contribute greatly to change the fore-aft asymmetry. Roberts (2006) pointed out that flagella have significant influence on the shape-asymmetry for the generation of the gravitactic torque. He also indicated that the effect of the flagella changed dynamically depending on their bending form during a beat cycle. These may support the idea that the fore-aft shape asymmetry could change in close relation to the alteration of the mode of flagellar beating, such as the modification of the coordinated beating of *cis*- and *trans*-flagella (Rüffer and Nultsch, 1987).

Results shown in Fig. 7 indicate that the changes in the tactic features discussed above seem to occur reversibly depending on the intensity of the light of phtosynthetically active wave length. Sineshchekov et al. (2000) reported that red light affected the intensity of negative gravitaxis. When irradiated by red light, negative gravitaxis became intense or less marked, depending on the initial levels of tactic behavior. Williams and Bees (2011a), however, reported that the onset pattern wavelength was unresponsive to changes in red light (660 nm) with the intensity much larger than that used in the present study. It should be stressed that the red-light-induced alteration of the pattern wavelength was found specifically in the SS2, neither in Onset nor in the SS1. It is therefore likely that the pattern transition response may occur in association with the physiological changes of the cell responsible for the sensitivity to the illumination intensity, which may be achieved after the transition. Wakabayashi et al. (2010) reported that the phototactic response of *Chlamydomonas* was influenced by redox poise of the cell. It might be possible that changes in the intracellular environment related to photosynthesis trigger the changes in gravitaxis and/or gyrotaxis which may result in the changes in the bioconvection pattern wavelength.

Enhancement of gyrotaxis could be explained in terms of the swimming velocity of the cell. The higher the swimming velocity, the larger number of the cell tends to accumulate in the axis of the downward axial flow. This may accelerate the cell suspension to trigger the pattern transition response. In fact, in Williams and Bees (2011b), three linearized models are proposed for photo-gyrotactic bioconvection, which include both gyrotaxis and phototaxis. In one of their models (Model 1), phototaxis is included by modeling cell swimming speed as a function of light intensity. In this model, the mean cell swimming direction is determined separately by balancing

gravitational and viscous torques in a stochastic formulation (Williams and Bees, 2011b). Their result indicates that varying the light intensity (and thus the cell swimming speed) did have a significant effect on the pattern wavelength (Williams and Bees, 2011b, Fig. 8). Sineshchekov et al. (2000) reported that red light affected the velocity of free-swimming *Chlamydomonas*. These facts suggest a possible role of swimming velocity in the pattern transition response and the subsequent changes in the pattern wavelength, although we have not so far observed in the bioconvection pattern the increase in the swimming velocity of the cell.

There might be other mechanistic explanations. SS1 and SS2 are both stable convection systems, presumably with SS2 being more stable than SS1. The transition from SS1 to SS2 could be triggered by number density fluctuations in the medium. Another possibility may be that cell motility is stimulated during the initial mixing leading to SS1, then flipping to SS2 as swimming velocity relaxes.

In the present paper, we present the dynamic behavior of the bioconvection pattern of *Chlamydomonas* that has not been imagined so far. The pattern transition response suggests that bioconvection pattern has a potential to reorganize its convection structure, even when seemingly stable. This ability of the reorganization might allow bioconvection to sharply respond to environmental cues. Such responsiveness would be assumed from the fact that pattern wavelength changed reversibly depending on the illumination intensity.

The possibility has been pointed out that bioconvection could play some roles in physiological processes of microorganisms, such as proliferation, germination, nutrient uptake, gas transport or photosynthesis (Noever et al., 1994; Turner, 2000; Ochiai et al., 2011; Williams & Bees, 2011a), although the conclusions of the empirical

studies do not still seem to reach an agreement. The experimental study on proliferation claims negative results (Janosi et al., 2002), while the hydrodynamic observation and calculation show that formation of bioconvection should promote oxygen transport (Tuval et al., 2005).

For the assessment of the biological function of bioconvection, dynamic features of the steady-state pattern presented in the present paper would be informative. Further studies on the details of the long-term behavior of bioconvection including the pattern transition response should be required to clarify the crucial roles of the collective motion in the activity of microorganisms.

Acknowledgement

This work was supported in part by a grant from the ISAS/JAXA Space Utilization Research Working Group. A.K. is supported by the Research Fellowship of the Japan Society for the Promotion of Science for Young Scientists.

Author Contributions

A.K. and Y.M. designed the research. A.K. and C.H. conducted the experiments and analyzed the data. A.K. and Y.M. fabricated the experimental equipment. S.A.B. made the tools for the image analysis. A.K., Y.M. and S.A.B. wrote the paper.

The authors declare no competing interests.

Figure Legends

Fig. 1. Experimental setup of two-axis observation. Specimens in an experimental chamber of 3 × 3 × 40 mm were observed with two CCD cameras simultaneously from the top and from the side. CCD: CCD camera; Ch: experimental chamber; SC: sharp cut filter SC-64 (λ>640 nm); Sl: slit; CCFL: cold cathode fluorescent lamp; Rec: recorder; Ver: vertical observation (side-view); Hor: horizontal observation (top-view).

Fig. 2. Long-term development of a typical bioconvection pattern of *Chlamydomonas reinhardtii*. A, snapshots of the bioconvection pattern (plan-view). Numbers indicate the time in minutes after the transfer of the cell suspension into the experimental chamber. B, long-term change of the pattern wave number obtained from the images shown in A. Dominant wave number (spatial frequency) calculated by the 2D-FFT analysis is plotted against the time after the transfer of the cell suspension. Three remarkable phases of the pattern formation focused in this paper, *Onset*, *Steady State 1* (SS1) and *Steady State 2* (SS2) are indicated. C, space-time plot demonstrating the transitional event of the bioconvection pattern of the bulk of the *Chlamydomonas* suspension. Time axis (abscissa) is common to that in B. Suspension depth: 4 mm; cell density: 1.0×10^7 cells/ml. Scale bars are as indicated. See Movie S1.

Fig. 3. Pattern wave numbers obtained from the images at the three remarkable phases. A, pattern wave numbers of *Steady State 1* (open circle) and *Steady State 2* (filled circle) are plotted as a function of the wave number of the *Onset* phase. B, pattern wave numbers of *Steady State 2* as a function of the wave number of *Steady State 1*. Pearson's correlation coefficient (R) of each plot is shown with p-value (p) and sample size (n).

Suspension depth: 4 mm; cell density: 1.0×10^7 cells/ml.

Fig. 4. Effects of suspension depth and cell density on the pattern wave number in the three phases of bioconvection. A, wave numbers of the *Onset* phase (mean ± S.D.) measured in four different density of cell suspension are plotted against the suspension depth. B, wave numbers of the *Steady State 1* (open symbol) and *Steady State 2* (filled symbol) measured in four different density of cell suspension are plotted against the suspension depth. The significance level of the trends (dependency) obtained by Kruskal-Wallis test is shown for each plot.

Fig. 5. Effect of cell density on the initiation time of pattern transition response. Time from the transfer of the suspension to the initiation of the transition (mean ± S.D.) are plotted as a function of the cell density of the suspension. The significance level of the trends (dependency) obtained by Kruskal-Wallis test is shown. Suspension depth: 4 mm.

Fig. 6. Two-axis view recording of the pattern transition response. A, snapshots of a bioconvection pattern obtained by the two-axis observation showing the images from the vertical observation (side-view, left column) and the horizontal observation (top-view, right column) with respect to the same time sequence from the start of the experiment (0 min) to steady-state pattern formation (25 min) following the pattern transition response (11-14 min). Faced triangles marked B to D indicate the positions from which space-time plots are made. B to D, space-time plots obtained from the portion of the vertical images (B and C from the top and the bottom portion, respectively) and the horizontal image (D). Scale bars, 5 mm. See Movie S2.

Fig. 7. Light intensity dependent changes in the wave number of the bioconvection pattern. A, Decrease in the wave number in response to the change of the illumination conditions from intermittent lighting (IL) to continuous lighting (CL) B, reversible changes in the wave number in response to the change of illumination conditions. C, effect of reduced light intensity on the wave number of the pattern before and after the pattern transition response. Two samples from the same batch were illuminated with and without a neutral density (ND) filter and simultaneously recorded. Open circles, the specimen illuminated with no ND filter (control); closed circles, the specimen illuminated with ND 0.3 filter (50 % of light was cut off). D, wave numbers of *Onset*, SS1 and SS2, and the time when the pattern transition response occurred. White bars, the specimen illuminated with no ND filter (control); black bars, the specimen illuminated with ND 0.3 filter. Mean ± standard deviation is shown.

Supplementary Movie Legends

Movie S1. Long-term behavior of bioconvection of *Chlamydomonas reinhardtii* showing the pattern transition response. The same specimen as shown in Fig. 2. Each side of the image is 20 mm. 90 min in real time.

Movie S2. Two-axis view of the pattern transition response. The same specimen as shown in Fig. 6. The upper part, side-view (vertical observation); The lower part, top-view (horizontal observation). 40 min in real time.

References

Akiyama, A., Ookida, A., Mogami, Y. and Baba, S.A. (2005). Spontaneous alteration of the pattern formation in the bioconvection of *Chlamydomonas reinhardtii*. *J. Jpn. Soc. Microgravity Appl.*, 22, 210 - 215.

Bees, M.A. and Hill, N.A. (1997). Wavelengths of bioconvection patterns. *J. Exp. Biol.* 200, 1515 – 1526.

Berg, H.C. (1993). *Random Walks in Biology Expanded Edition*, Princeton: Princeton University Press.

Childress, W.S., Levandowsky, M., and Spiegel, E.A. (1975). Pattern formation in a suspension of swimming microorganisms: equations and stability theory. *J. Fluid Mech*., 69, 591 - 613.

Ghorai, S. and Hill, N. A. (2000). Wavelength of gyrotactic plumes in bioconvection. *Bull. Math. Biol*. 62, 429-450.

Harashima, A., Watanabe, M. and Fujishiro, I. (1988). Evolution of bioconvection patterns in a culture of motile flagellates. *Phys. Fluids*, 31, 764-775.

Harris, E. (1989). *The Chlamydomonas Sourcebook*. San Diego: Academic Press.

Hopkins, M.M. and Fauci, L.J. (2002). A computational model of the collective fluid dynamics of motile micro-organisms. *J. Fluid Mech.*, 455, 149-174.

Hosoya, C., Akiyama, A., Kage, A., Baba, S.A. and Mogami, Y. (2010). Reverse bioconvection of *Chlamydomonas* in the hyper-density medium. *Biological Sciences in Space*. 24, 145-152.

Jánosi, I.M., Czirók, A., Silhavy, D., Holczinger, A. (2002). Is bioconvection enhancing bacterial growth in quiescent environments? *Environ Microbiol.* 4, 525-31.

Kage, A., Asato, E., Chiba, Y., Wada, Y., Katsu-Kimura, Y., Kubota, A., Sawai, S.,

Niihori, M., Baba, S.A., Mogami, Y. (2011). Gravity-dependent changes in bioconvection of *Tetrahymena* and *Chlamydomonas* during parabolic flight: increases in wave number induced by pre- and post-parabola hypergravity. *Zool. Sci*., 28, 206-214.

Kessler, J.O. (1985a). Co-operative and concentrative phenomena of swimming micro-organisms. *Contemp. Phys.* 26, 147-166.

Kessler, J.O. (1985b). Hydrodynamic focusing of motile algal cells. *Nature*, 313, 218-220

Kessler, J.O. (1986a). The external dynamics of swimming micro-organisms. In: *Progress in Phycological Research.* F. E. Round (Ed.), Vol. 4, pp. 257-307. Bristol: Biopress.

Kessler, J.O. (1986b). Individual and collective fluid dynammics of swimming cells. *J. Fluid Mech.*, 173, 191-205

Kitsunezaki, S., Komori, R., Harumoto, T. (2007). Bioconvection and front formation of Paramecium tetraurelia. *Phys Rev E Stat Nonlin Soft Matter Phys*. 76: 046301.

Levandowsky, M., Childress, W.S., Spiegel, A.E. and Hunter, S.H. (1975). A mathematical model of pattern formation by swimming microorganisms. *J. Protozool*. 22, 296 - 306.

Matsuda, A., Yoshimura, K., Sineshchekov, O.A., Hirono, M. and Kamiya, R. (1998). Isolation and characterization of novel *Chlamydomona*s mutants that display phototaxis but not photophobic response. *Cell Motil. Cytoskel.* 41, 353 – 362.

Mogami, Y., Ishii, J., Baba, S.A. (2001). Theoretical and experimental dissection of

gravity-dependent mechanical orientation in gravitactic microorganisms. *Biol Bull.* **201**, 26-33.

Mogami, Y., Yamane, A., Gino, A., and Baba, S.A. (2004). Bioconvective pattern formation of *Tetrahymena* under altered gravity. *J. Exp. Biol.* 207, 3349 - 3359.

Noever, D.A., Matsos, H.C. and Cronise, R.J. (1994). Bioconvective patterns, topological phase transitions and evidence of self-organized critical states. *Phys. Lett. A*, **194**, 295-299.

Ochiai, N., DragIila, M.I., and Parke, J.L. (2011). Pattern swimming of *Phytophthora citricola* zoospores: An example of microbial bioconvection. *Fungal Biology*, **115**, 228-35.

Roberts, A. M. (1970). Geotaxis in motile micro-organisms. *J. Exp. Biol.* 53, 687–699.

Roberts, A.M. (2006). Mechanisms of gravitaxis of *Chlamydomonas*. *Biol. Bull.*, 210, 78-80.

Rüffer, U., Nultsch, W. (1987). Comparison of the beating of *cis*- and *trans*-flagella of *Chlamydomonas* cells held on micropipettes. *Cell Motilit. Cytoskel.*, 7, 87–93.

Sineshchekov, O., Lebert, M., Häder, D.P. (2000). Effects of light on gravitaxis and velocity in *Chlamydomonas reinhardtii*. *J. Plant Physiol.* 157:247-54.

Turner, J.S. (2000). *The Extended Organism. The Physiology of Animal-Built Structures.* Cambridge: Harvard University Press.

Tuval, I., Cisneros, L., Dombrowski, C., Wolgemuth, C.W., Kessler, J.O., Goldstein, R.E. (2005). Bacterial swimming and oxygen transport near contact lines. *PNAS*, 102, 2277-82.

Wager, H. (1911). The effect of gravity upon the movements and aggregation of *Euglena viridis*, Ehrb., and other micro-organisms. *Phil. Trans. R. Soc. Lond. B*, 201, 333 – 390.

Wakabayashi, K., Misawa, Y., Mochiji, S. and Kamiya, R. (2010). Reduction-oxidation poise regulates the sign of phototaxis in *Chlamydomonas reinhardtii*. *PNAS*, 108, 11280-11284.

Williams, C.R. and Bees, M.A. (2011a). A tale of three taxes: photo-gyro-gravitactic bioconvection. *J. Exp. Biol*. 214, 2398-2408

Williams, C.R. and Bees, M.A. (2011b). Photo-gyrotactic bioconvection. *J. Fluid Mech.* doi:10.1017/jfm.2011.100, 1-46.

Yamamoto, Y., Okayama, T., Sato, K. and Takaoki, T. (1992). Relation of pattern formation to external conditions in the flagellate, *Chlamydomonas reinhardtii*. *Eur. J. Protistol.* 28, 415 – 420.

Yoshimura, K., Matsuo, Y. and Kamiya, R. (2003). Gravitaxis in *Chlamydomonas reinhardtii* studied with novel mutants. *Plant Cell Physiol.* 44, 1112-1118.

Fig. 1

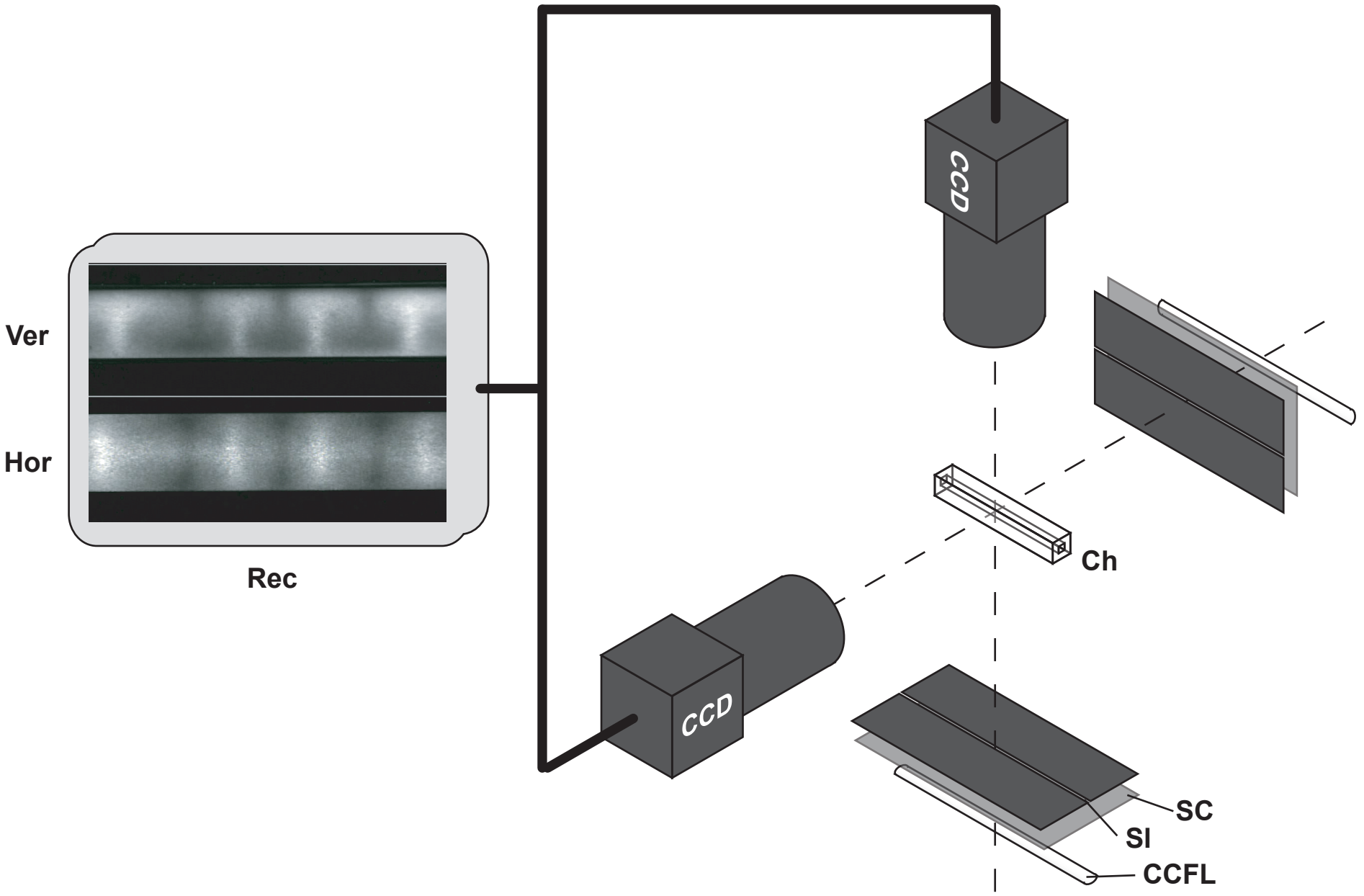

Fig. 2

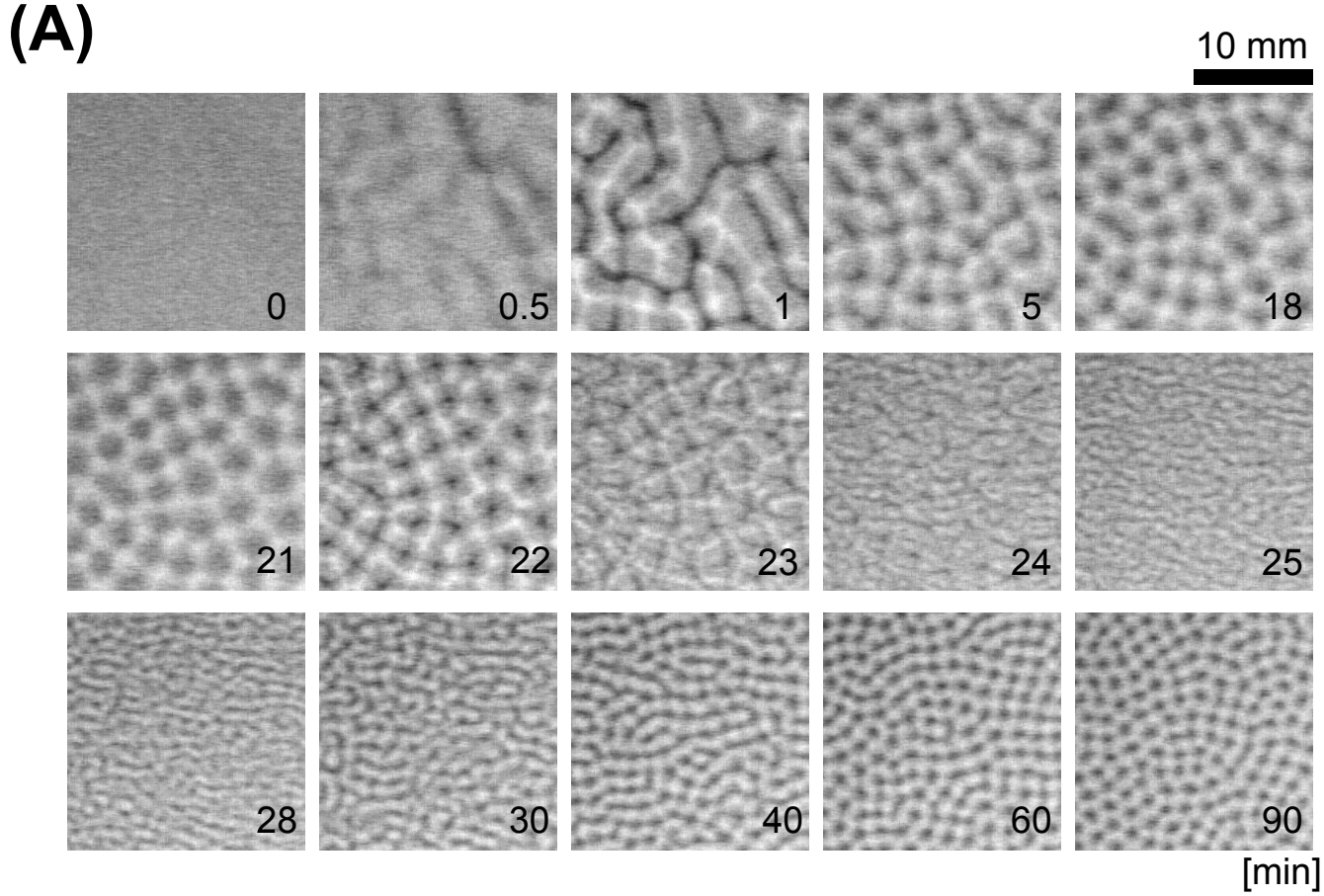

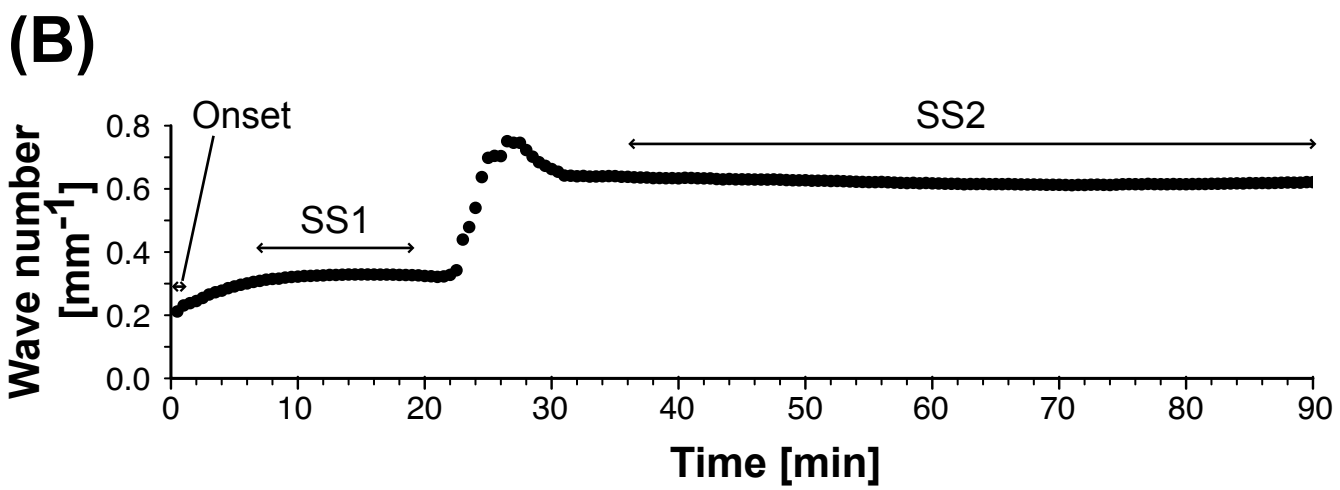

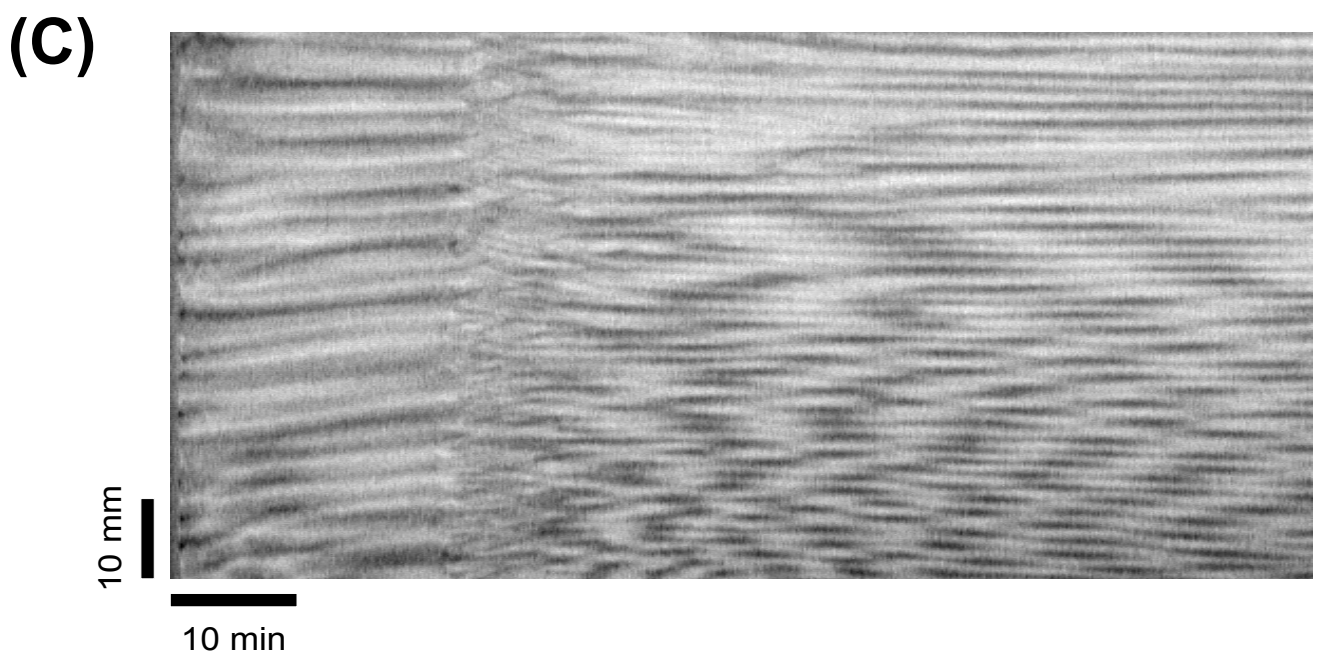

Fig. 3

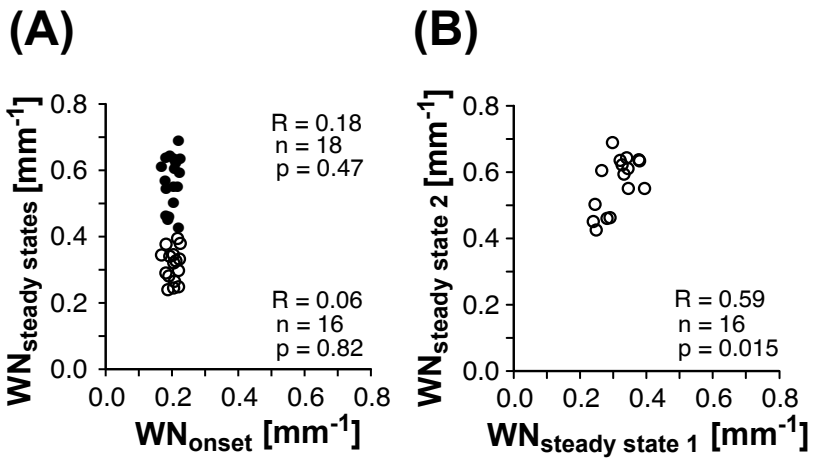

Fig. 4

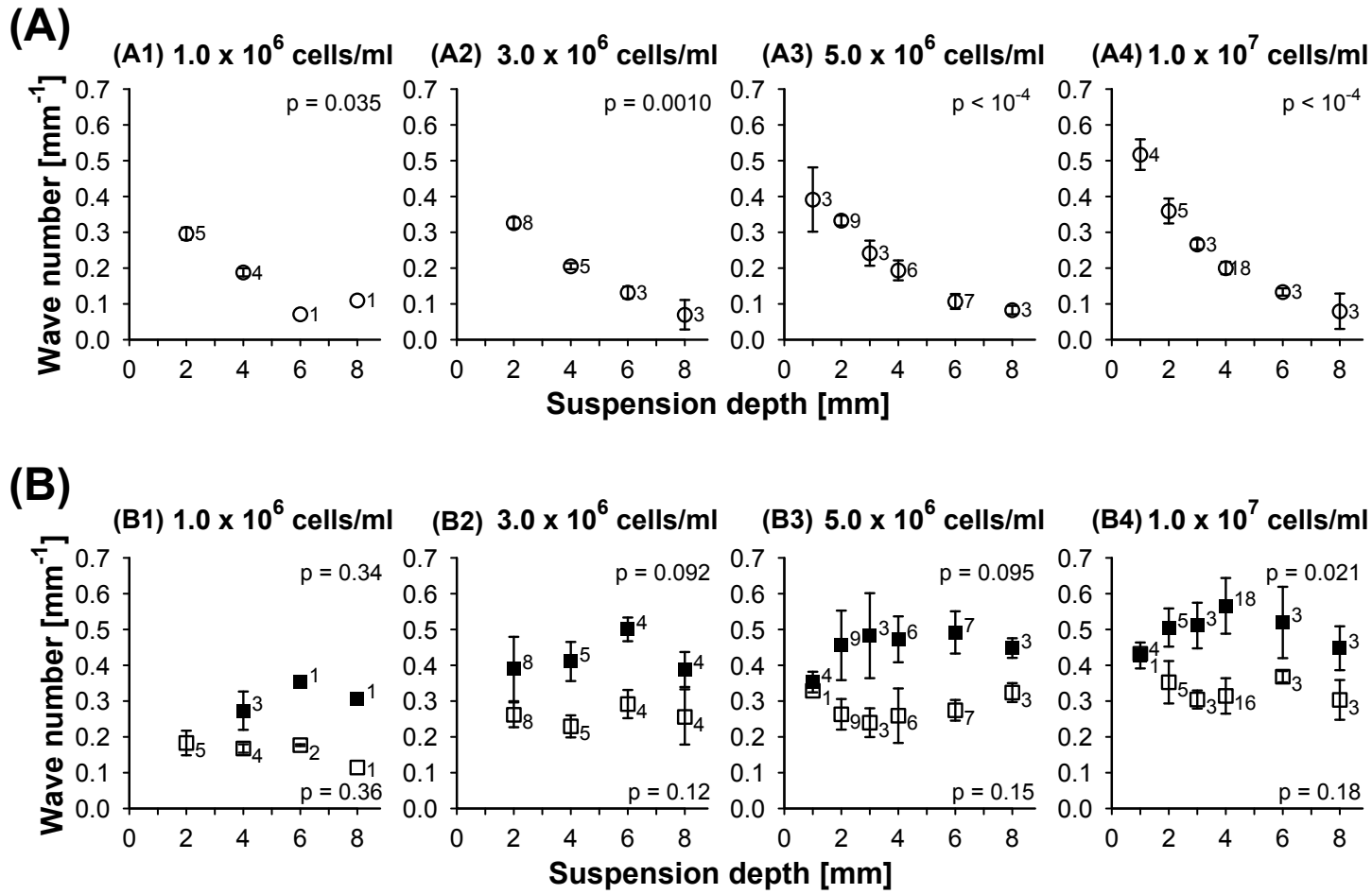

Fig. 5

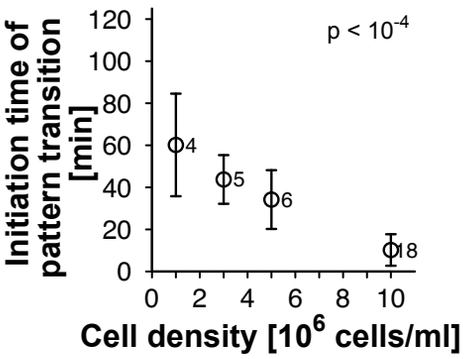

Fig. 6

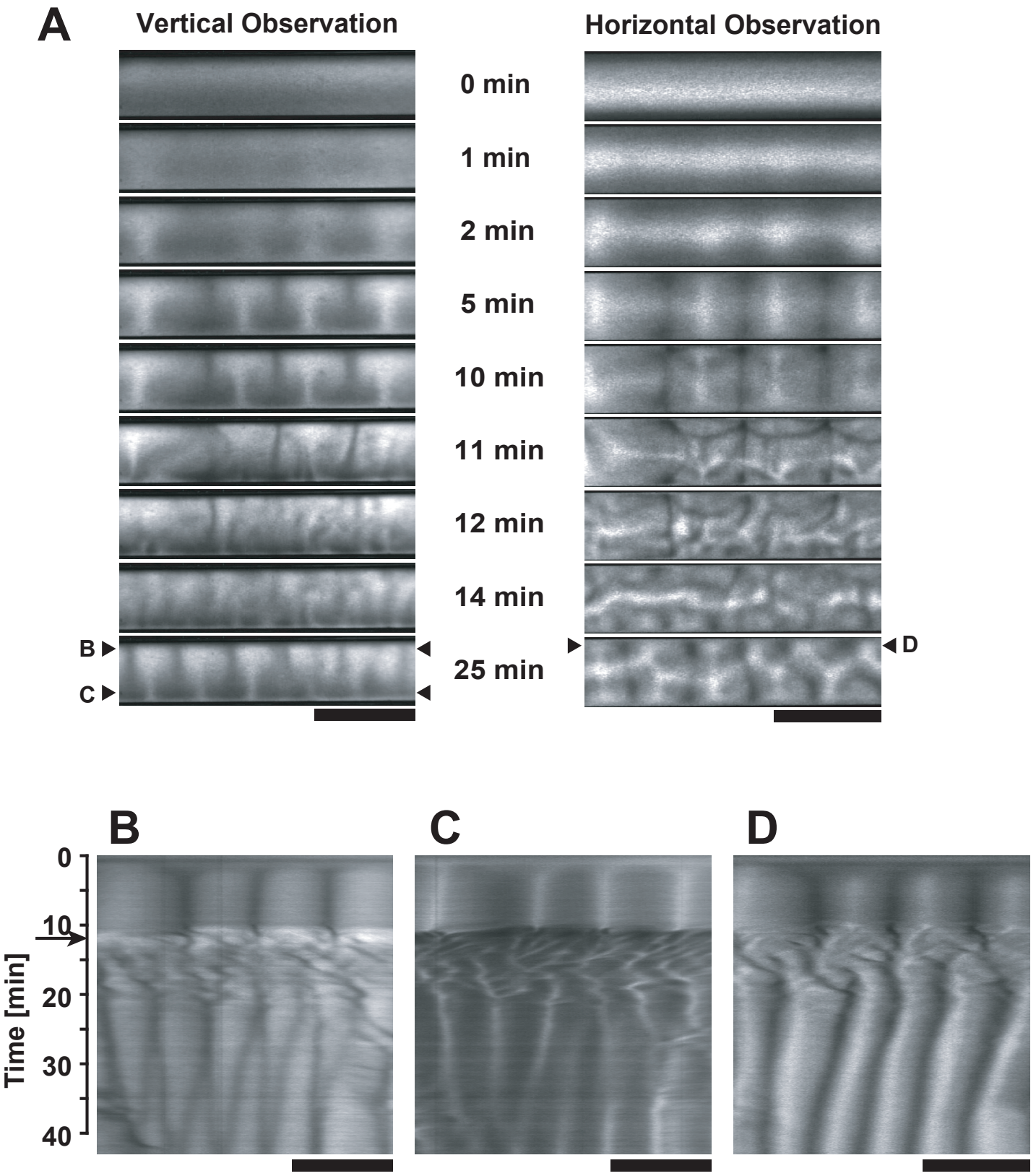

Fig. 7